HHS Public Access

Author manuscript

Exp Hematol. Author manuscript; available in PMC 2024 December 01.

Published in final edited form as:

Exp Hematol. 2023 December ; 128: 38–47. doi:10.1016/j.exphem.2023.09.003.

Physiological and Regenerative Functions of Sterile Alpha Motif Protein-14 in Hematopoiesis

Meg A. Schaefer[1], **Pooja Roy**[1], **Srinivas Chava**[1], **Ainsley Meyerson**[1], **Andrew L. Duncan**[1], **Linda Chee**[1], **Kyle J. Hewitt**[1,*]

[1] Department of Genetics, Cell Biology and Anatomy, University of Nebraska Medical Center, Omaha, NE, 68198, United States

Abstract

Sterile alpha motif domain-14 (Samd14) protein expression increases the regenerative capacity of the erythroid system. In a critical window of acute erythroid regeneration, *Samd14* is transcriptionally upregulated and promotes cell signaling via the receptor tyrosine kinase Kit. We generated a hematopoietic-specific conditional Samd14 knockout mouse model (Samd14-CKO) to study the role of Samd14 in hematopoiesis. The Samd14-CKO mouse was viable and exhibited no steady-state hematopoietic phenotype. Samd14-CKO mice were hypersensitive to 5-fluorouracil, resulting in more severe anemia during recovery and impaired erythroid progenitor colony formation. Ex vivo, Samd14-CKO hematopoietic progenitors were defective in their ability to form mast cells. Samd14-CKO mast cells exhibited altered Kit/SCF, IL-3/IL-3R signaling, and less granularity compared to Samd14-FL/FL cells. Our findings indicate that Samd14 promotes both erythroid and mast cell functions. The Samd14-CKO mouse phenotype exhibits striking similarities to the $Kit^{W/W\text{-}v}$ mice, which carry Kit mutations resulting in reduced tyrosine kinase-dependent signaling, causing mast cell and erythroid abnormalities. The Samd14-CKO mouse model is a new tool for studying hematologic pathologies involving Kit signaling.

Keywords

erythropoiesis; regeneration; mast cell; receptor tyrosine kinase signaling

Introduction

Samd14 promotes signal pathway duration and intensity in hematopoietic stem/progenitor cells (HSPC) and erythroid progenitors downstream of stem cell factor (SCF) and erythropoietin (Epo) stimulation during regenerative erythropoiesis (1,2). Samd14 shares

* To whom correspondence should be addressed. Tel: (402) 559-4689 kyle.hewitt@unmc.edu.
Permanent Address: Department of Genetics, Cell Biology & Anatomy, University of Nebraska Medical Center, 985805 Nebraska Medical Center, Omaha, NE 68198-5805

CONFLICT OF INTEREST
None

homology with neurabin proteins (PPP1R9A and PPP1R9B) which promote cell signaling and survival in neurons (3). Neurabin mechanisms-of-action include signaling complex recruitment to actin filaments and controlling specificity of signaling pathway activation within certain cell subtypes (4,5). We previously characterized a Samd14-Enhancer deletion mouse (Samd14$^{\Delta Enh/\Delta Enh}$) that lowered Samd14 levels in erythropoietic progenitors and reduced anemia-dependent Kit receptor tyrosine kinase (RTK) signaling (1). In stress erythroid precursors isolated from anemic mouse spleens, both the sterile alpha motif (SAM) and capping protein binding (CPB) domains of Samd14 are required for maximal Kit signaling via MAPK and PI3K/Akt pathways, promoting cell survival and colony forming activity of stress-activated erythroid precursors (2,6). These data support an anemia recovery model in which anemia-dependent Samd14 transcription increases Kit signaling to promote erythroid cell survival and progenitor activity.

The Kit receptor and its ligand, stem cell factor (SCF), control hematopoietic lineage development and function (7). Kit activating mutations are found in systemic mastocytosis (8), leukemia (9,10), and gastrointestinal stromal tumors (11). Loss-of-function Kit or SCF mutations in mice influence the development and/or function of erythroid and mast cell populations, as well as hematopoietic progenitors, melanocytes, and germ cells (12–14). Kit knock-in mutant mouse models have normal physiological hematopoiesis but are sensitive to acute anemia stress induced by phenylhydrazine or 5 fluorouracil (5-FU) (15). One of the least severe naturally-occurring Kit mutations to be described, a valine to methionine mutation at residue 831, causes mild anemia and defective mast cell development, as evidenced by *ex vivo* mast cell differentiation assays (16). Since anemia and mast cell defects are still found in mild Kit loss-of-function alleles, these phenotypic traits are sensitive to Kit signaling perturbations. Kit mutant mice characterizations provide valuable in vivo comparisons to facilitate investigations of structural elements necessary for downstream signal transduction, and the role of receptor tyrosine kinase mechanisms in cellular differentiation.

Samd14 is a direct target gene of the GATA2 transcription factor expressed in megakaryocyte-erythroid progenitors and erythroid precursors (17,18). *Gata2* and *Samd14* transcription are both controlled by conserved E-box-spacer-GATA composite element enhancers. The study of these and related enhancers established a foundation for defining a GATA2 and anemia-activated genetic network as potentially critical nodes (1,19). Despite evidence linking Samd14 to hematopoiesis and erythropoiesis, no gene knockout mouse has been previously described. We generated a hematopoietic-specific conditional knockout mouse model of Samd14 to study its role in hematopoietic cells. Samd14 conditional knockout (CKO) mice exhibited defective mast cell differentiation, and mice were hypersensitive to myelo-ablative 5-FU treatment. Beyond known roles for Samd14 in promoting Kit signaling – and parallels between this mouse phenotype and Kit loss-of-function – we found that Samd14 also promoted signaling through the mast cell-promoting IL-3 signaling pathway. This new mouse model permits investigations into the requirement of Samd14 in hematologic diseases, including systemic mastocytosis, chronic anemias, and leukemias, as well as addressing Samd14 expression and cell autonomous vs. non-cell autonomous functions in contexts of hematologic malignancy.

Methods

Mice

Samd14$^{fl/fl}$ mice in C57BL/6 mice were generated using Easi-CRISPR (20), and crossed with E2A^{Cre} or Vav^{iCre} mice (Jackson Labs). All mouse experiments were approved by Institutional Animal Care and Use Committee of University of Nebraska Medical Center in accordance with National Institutes of Health guidelines.

Flow Cytometry

Total bone marrow and spleen cells from 8–12 week old mice were resuspended in PBS with 2% FBS and passed through a 25 um cell strainer to obtain singe cell suspensions. Surface proteins were detected with pre-conjugated antibodies specific for surface proteins CD71 (R17217), Ter119 (116212), Kit (clone 2B8) (105814), FcƐr1α (Clone MAR-1), CD11b (Clone M1/70), CD16/32 (Clone 93), Integrin-β7 (Clone FIB504), Mac1, Gr.1 (Clone RB6–8C5), Thy1.2 (Clone 53–2.1), CD19 (Clone 6D5), Annexin V (640917) for 30 mins at 4°C (all from Biolegend). Cells were resuspended with either DAPI or Draq7 (Biolegend) viability dyes as required and analyzed on LSR Fortessa (BD Biosciences). Fluorescence Activated Cell Sorting for GFP+ cells or CD71− and Ter119-fractionation was conducted on a FACSAria II (BD Life Sciences). Data was analyzed with FlowJo v10.6.2.

5-Fluorouracil

Myeloablation was induced by a single dose (250 mg/kg) of 5-flourouracil (MilliporeSigma, F6627) administered intraperitoneally. Blood samples were collected by retro-orbital bleeding (~100 μl per collection), and hematologic parameters were quantified on a HemaVet complete blood count (CBC) instrument (Drew Scientific).

RBC Lifespan

Cells in peripheral circulation were biotinylated by retro-orbital injection of 3 mg EZ-Link Sulfo-NHS-Biotin (Thermo Scientific) dissolved in PBS. On days 1, 8, 15, 22 and 29 post injection, recipients were bled via the pedal vein. Biotinylated RBCs were detected by flow cytometry using a combination of APC anti-mouse Ter119 (BioLegend) and PE/Cyanine7 Streptavidin (BioLegend) antibodies. 5 WT and 5 CKO mice were analyzed.

Mast Cell Differentiation and Culture

Bone marrow flushed from 8–16-week-old Samd14-FL/FL and Samd14-CKO mice was resuspended in mast cell differentiation media (DMEM with 10% fetal bovine serum (FBS), 0.14 mM β-mercaptoethanol, L-glutamine, and 10 ng/mL IL-3). Cells were cultured for 14 days and maintained at 0.1–0.5×10^6/mL. After 14 days, cells were cultured for 14 days with conditioned mSCF Chinese Hamster Ovary media (1:1000). Alternatively, flushed bone marrow was lineage depleted with biotin-conjugated antibodies and MojoSort streptavidin-conjugated magnetic nanobeads (Biolegend): anti-mouse CD3e (clone 145–2 C11), anti-mouse CD11b (clone M1/70), anti-mouse CD19 (clone 6D5), anti-mouse CD45R (B220) (clone RA3–6B2), anti-mouse Gr-1 (clone RB6-C5), anti-mouse Ter119. After lineage depletion, cells were stained with PE-Cy7-conjugated anti-Kit antibody and sorted

for live (DAPI$^-$), Kit$^+$ cells. After sort, cells were resuspended in mast cell differentiation media containing 10ng/mL IL-3 and 1:1000 conditioned mSCF media and cultured for 14 days.

BMCP Isolation and CFU Assays

Spleens from 8–16-week-old WT or Mut mice were dissociated, resuspended in PBS with 2% FBS and filtered through a 25 μm cell strainer. Lineage-negative cells were obtained through lineage depletion and cells were stained and sorted for Kit$^+$ SCA-1$^-$, CD16/32$^+$ Integrin-β7$^+$ BMCPs. 2,000 BMCPs/mL were mixed with Methocult M3234 (STEMCELL Technologies) containing 10ng/mL IL-3 and 1:1000 mSCF. Cells were plated in replicate 12-well plates (1,000 cells in 0.5 mL). BMCPs were counted 7 days after plating.

For erythroid BFU-E and CFU-E assays at 10 days post-5-FU, bone marrow was isolated from WT and CKO mice. Cells were lineage depleted by incubating in biotin-conjugated anti-CD34ε, anti-CD11b, anti-CD19, anti-CD45R, anti-Gr-1, anti-Ter119 and anti-CD71 antibodies (1:200 in PBS containing 5% FBS), followed by incubation with Streptavidin-conjugated magnetic beads (MojoSort - BioLegend). Methylcellulose media (MethoCult GF M3434 – STEMCELL Technologies) contained SCF, Epo, IL-3 and IL-6 (1250 cells/replicate, 3 replicates per mouse). CFU-E colonies were counted 3 days after plating while BFU-E colonies were counted after 6 days.

Western blotting

Mast cells were isolated with biotin-conjugated FcЄr1α (Clone MAR-1) and MojoSort streptavidin-conjugated magnetic nanobeads. Proteins were boiled in SDS buffer (25 mM Tris, pH 6.8, 2% β-mercaptoethanol, 3% SDS, 5% bromophenol blue, 5% glycerol) for 10 min, resolved by SDS-PAGE using Pierce ECL (Thermo Scientific). Primary antibodies: polyclonal anti-Samd14 (1), anti-β-actin (Cell Signaling Technology). Secondary antibodies: goat-anti-mouse-IgG-HRP, goat-anti-rabbit-IgG-HRP (Jackson Labs).

Wright-Giemsa Staining

Cells from 2-week mast cell differentiation cultures were collected, stained, and sorted for Kit$^+$ FcЄr1α$^+$ mast cells. Sorted cells were cytospun onto slides, stained with Wright-Giemsa stain, and imaged at 40x. The number of granulated versus non-granulated mast cells was quantitated by scoring for the presence/absence of granules in 100 cells per slide.

Toluidine Blue Staining

Ears from WT and Mut mice were cut at the base of the ear and fixed at 4°C in 4% paraformaldehyde (PFA) overnight. Ears were paraffin-embedded and sectioned at 6μm and 8μm, dehydrated in ethanol, and stained with toluidine blue (Sigma-Aldrich) for 2 minutes. Slides were imaged at 20x. Mast cells were counted on each section for every ear analyzed, and ImageJ measure function was used to determine the number of mast cells/mm^2.

Phospho-flow Cytometry

Mast cells from 2-week differentiated cultures were labeled with biotin-conjugated anti-FcЄr1α antibody and isolated using streptavidin-conjugated magnetic nanobeads. After 16

hours serum starvation in mast cell media without cytokines at 37°C, cells were washed and resuspended in Tyrodes buffer (10mM Hepes, 130mM NaCl, 5mM KCl, 1.4 mM CaCl2, 1mM MgCl2, 5.6mM glucose, 0.1% BSA). Cells were stimulated with 10ng/mL SCF or PBS for 5 minutes, fixed in 2% PFA for 10 min at 37°C, and permeabilized in 95% methanol overnight at −20°C. Cells were stained with the rabbit anti-phospho (Thr202/Tyr204) p44/42 ERK1/2 (p-ERK) antibody (9101; Cell Signaling), then incubated with APC-conjugated goat anti-rabbit, and anti-Kit, and analyzed using the BD LSR II flow cytometer. Gates were drawn based on fluorescence minus one controls. pERK levels were calculated by MFI using FlowJo v10.6.2 (BD Life Sciences). Fold change was determined as activation of SCF-treated samples relative to vehicle-treated controls.

SCF-Induced Passive Cutaneous Anaphylaxis

Mice were anesthetized, and ear thickness was measured using a dial thickness gauge (Peacock). 25 ul of PBS alone was injected into the left ear pinnae, and PBS containing 50 μg/mL of recombinant mouse SCF (R&D Systems) was injected into the right ear pinnae of each mouse with a 30G x ½ needle. Ear thickness was measured again after 2 hours. Changes in ear thickness were determined as post-injection ear thickness minus initial ear thickness for each ear.

Results and Discussion

Erythropoiesis in Samd14-CKO mice is normal at baseline but defective during regeneration.

Human and mouse gene expression databases reveal high mRNA expression of SAMD14 in hematopoietic stem/progenitor cells (HSPCs), common myeloid progenitors (CMPs), megakaryocyte-erythrocyte progenitors (MEPs), and throughout the erythroid lineage, as well as in the central nervous system. In red blood cell precursors but not $Lin^{-}Sca1^{+}Kit^{+}$ or brain tissues, an intronic Samd14 enhancer (Samd14-Enh) is required for transcriptional activation of Samd14 (1). To understand the role of Samd14 more broadly in the hematopoietic system, we generated a transgenic mouse containing LoxP sites flanking intron 3 (Figure 1A). Crossing to the hematopoietic-specific Vav-Cre line resulted in exon 3 excision in bone marrow and peripheral blood (Figure 1B). Western blotting revealed a loss of Samd14 protein in bone marrow isolated $Samd14^{fl/fl}$ (WT) mice or $Samd14^{fl/fl;Vavi\text{-}Cre}$ (Samd14-CKO) (Figure 1C). Heterozygous crosses of $Samd14^{fl/-}$ mice and $Samd14^{CKO/+}$ or heterozygous crosses of germline deletion of Samd14 exon 3, produced offspring of normal Mendelian ratios (Figure 1D), indicating that Samd14 expression was not required for embryogenesis. In peripheral blood from eight week-old Samd14-FL/FL and Samd14-CKO mice, complete blood count (CBC) hematological parameters did not differ (Figure 1E). In skin and spleen, no significant differences were seen in mast cell numbers in Samd14-FL/FL vs. Samd14-CKO mice (Figure 1F). The percentages of cells at distinct stages of erythroid maturation ($CD71^{+}Ter119^{+}$ and $CD71^{-}Ter119+$) (Zhang et al., 2003) were unaltered in Samd14-CKO bone marrow and spleen (Figure 1G). B-cell ($CD19^{+}$) percentages were marginally decreased in Samd14-CKO (Figure 1G). Samd14-CKO in the steady state hematopoietic system, therefore, has minimal impact on bone marrow, spleen or peripheral blood cellular parameters.

Cell signaling via the Kit proto-oncogene is promoted by Samd14 expression in specific contexts of regenerative erythropoiesis (1). Similarly, among the hematologic phenotypes in mice carrying mutations in the Kit locus, and particularly in mutant strains that lack baseline erythropoietic defects, they exhibit delayed regenerative erythropoiesis (15). Therefore, we next tested whether loss of Samd14 is important for hematopoietic regeneration following 5-fluoruracil (5-FU) myeloablation. After administering 250 mg/kg 5-FU, mice were monitored for signs of anemia. At days 8 and 11 post-treatment, RBCs/uL in peripheral blood was 1.5-fold and 1.4-fold lower in CKO vs. Samd14$^{FL/FL}$ mice, respectively (Figure 2A). Hemoglobin (g/dL) was 1.6-fold and 1.3-fold lower in CKO vs. Samd14$^{FL/FL}$ mice at the same respective time points (Figure 2B). Percentage of peripheral blood hematocrit was also decreased in CKO vs. Samd14$^{FL/FL}$ mice at days 8 and 11 post-treatment, 1.6-fold ($p=0.0005$) and 1.3-fold ($p=0.016$) (Figure 2C). To test whether Samd14 expression was promoting RBC lifespan in peripheral blood, possibly contributing to the regeneration-specific phenotype, we labeled RBCs in Samd14$^{FL/FL}$ and CKO mice with biotin and monitored for 29 days. No significant differences were observed in the labeled RBCs at 8–29 days (Figure 2D). To test whether 5-FU injection altered erythroid progenitor activity in Samd14-KO mice, we isolated bone marrow from mice at 10 days post-5-FU injection and conducted colony formation assays. These data showed 1.6-fold fewer BFU-E and 1.78-fold fewer CFU-E colonies in mutant compared to WT mice. Thus, defective stress hematopoiesis in Samd14 knockout mice was associated with decreased progenitor activity.

Samd14 promotes mast cell differentiation.

A signal from the Kit receptor is needed for erythroid precursor survival/proliferation and in mast cells. The GATA2 transcription factor – which regulates Samd14 expression – is a critical driver of mast cell identity (21–24). Given overlapping Samd14 and Kit activities in knockout mouse models, and the importance of Kit and GATA2 in mast cell development and function (25), we examined the ability of Samd14-CKO hematopoietic progenitors to differentiate to mast cells. *Ex vivo* mast cell differentiation and culture systems provide a robust and definitive readout for genetic requirements of Kit and GATA2 in mast cells, among others (16,21). To examine if Samd14 is required for mast cell differentiation, total bone marrow was isolated from Samd14-FL/FL and S14-CKO mice. Bone marrow cells were cultured in IL-3-containing media for 14 days and IL-3- and SCF-containing media from days 15–28 (Figure 3A), according to published protocols (26). Western blotting of sorted mast cells (FcεR1α^{+}Kit^{+}) after 28 days culture confirmed that Samd14 is highly expressed in mast cells and absent in Samd14-CKO cells (Figure 3B). Cell cultures were analyzed by flow cytometry at days 7, 14, 21, and 28 of differentiation for the percentage of Kit^{+} FcεR1α^{+} cells (Figure 3C). Whereas the mast cell percentages were approximately equal after 7 days, day 14 cultures from Samd14-CKO bone marrow had 10.7% fewer mast cells than WT ($p=0.009$). By day 28, 75.2% of WT cultures were mast cells, while 31.0% of S14$^{-/-}$ cultures were mast cells ($p=0.0003$). Thus, Samd14 promotes mast cell differentiation.

Next, we examined whether Samd14-CKO cells were differentiating to alternative lineages instead of mast cells. We established a new method for differentiating mast cells from primary bone marrow, which proved to be more efficient and resulted in fewer dead/

dying cells. Total bone marrow was lineage depleted with magnetic beads, sorted for Kit^+ cells, and cultured in IL-3- and SCF-containing media for 14 days (Figure 4A). Flow cytometry was performed on day 14 to quantitate percentages of mast cells (Kit and FcεR1α), granulocytes ($CD11b^+Gr1^+$) and monocytes ($CD11b^+Gr1^-$) in cultures. This analysis revealed that the 61.7% of the culture that was not mast cells was either monocytes ($CD11b^+$, $GR\text{-}1^-$) or granulocytes ($CD11b^+$, $Gr1^+$) (Figures 4B and 4C). We observed a 1.6-fold increase in the percentage of monocytes in Samd14-CKO cells compared to Samd14-FL/FL cells (p=0.012), and a 1.7-fold increase in the percentage of granulocytes (p=0.028) (Figure 4C). To test if cellularity differences in Samd14-CKO cultures were related to changes in cell survival (which has been observed in the erythroid lineage), we stained cells with the apoptotic marker Annexin V. An increase (18.9% to 22.1%) in early apoptosis was observed in $FcεR1A^+Kit^+$ Samd14-CKO mast cells (p=0.027) but not monocytes and granulocytes (Fig 4D and 4E), revealing that loss of Samd14 decreases mast cell survival. Since lack of Samd14 resulted in more *ex vivo* monocyte differentiation at the expense of mast cells, Samd14 expression levels may guide cell fate of multipotent progenitors. These results are consistent with models of mast cell lineage specification that relies on high Kit signaling activity (27).

To determine whether mast cell progenitor numbers in Samd14-CKO mice could explain this phenotype, we conducted immunophenotypic and functional profiling of progenitors. A bipotent basophil-mast cell progenitor (BMCP) expressing Integrin beta 7 (Itgβ7) and FcγR is resident in mouse bone marrow and spleen (28). We isolated spleens from $S14\text{-}^{FL/FL}$ and $S14\text{-}^{CKO}$ mice, lineage depleted, and analyzed the number of BMCPs (Fig 4F). There were no significant differences in BMCP percentages between genotypes in spleen (Fig 4G). FACS-purified spleen BMCPs were isolated and grown in IL-3 and SCF-containing semisolid media for 7 days. The number of colonies formed by Samd14-CKO BMCPs was 1.4-fold (p=0.0002) lower compared to Samd14-FL/FL, indicating that Samd14 promotes BMCP colony formation (Fig 4G). Taken together, these results reveal that Samd14 plays a role in multiple facets of mast cell differentiation, including lineage commitment, mast cell survival, and progenitor activity resulting in defective mast cell differentiation.

Mast cell signaling pathways and activation are Samd14-dependent.

To examine whether Samd14 mediated Kit receptor signaling in mast cells, we bead sorted $FcεR1α^+$ mast cells after 14 days in culture, then serum-starved and stimulated with the Kit ligand SCF (Figure 5A). Phosphorylated ERK (pThr202/pTyr204 - pERK) levels were monitored by intracellular antibody staining and flow cytometry. This analysis revealed a 1.5-fold (p=0.006) decrease in SCF-mediated pERK in Samd14-CKO mast cells versus Samd14-FL/FL mast cells (Figure 5B). Among the notable observations from longer term mast cell differentiation protocols (Figure 3C), mast cell percentages were lower at day 14 before adding SCF to the media, suggesting that Samd14 may promote IL-3 signaling. While IL-3 is not essential for mast cell lineage development, it enhances mast cell production during development and ex vivo differentiation (29,30). When mast cells were stimulated with IL-3, pERK levels were 2.3-fold lower in S14-CKO cells compared to WT cells (p=0.003) (Figure 5C). These results indicate signaling defects in mast cells lacking Samd14. Intriguingly, prior work has linked Samd14 overexpression in mast cells to an

altered secretory phenotype (31). Samd14 may have a general role in human and mouse mast cell signaling.

After observing that Samd14 promoted mast cell differentiation, survival, progenitor activity, and cell signaling, we next tested whether Samd14 controlled mast cell function. Both human and mouse mast cells can be activated in vivo using a subcutaneous SCF injection (32,33). To investigate whether SCF could initiate mast cell activation and degranulation in Samd14-CKO mast cells *in vivo*, we injected the ears of Samd14-CKO and S14-Fl/Fl mice with either SCF or PBS-alone and measured changes in ear thickness as an indicator of mast cell-induced tissue inflammation. Samd14-FL/FL mice exhibited an expected increased inflammation following SCF injection, but no corresponding increase was observed in Samd14-CKO mice (Fig 5D). These results indicate that Samd14 is needed for effective SCF-mediated mast cell degranulation in vivo. Tissue-resident mast cells are responsible for immunologic reactions through the binding of IgE and crosslinking of their FcЄR1 receptor. Upon stimulation, histamine, prostaglandins, and cytokines are released from mast cell granules causing inflammation and immune cell infiltration (34). To examine mast cell granularity after differentiation, we sorted mast cells after 14 days in culture, stained them with Wright-Giemsa, and quantified the number of granulated mast cells (Figure 5E). 24.3% of WT mast cells contained granules, while only 7.9% of S14-CKO mast cells were granulated (p=0.016) (Figure 5F). Therefore, loss of Samd14 decreased mast cell granule formation. We next isolated RNA from sorted mast cells to examine gene expression levels of granule-containing proteins. Mast cell protease 4 (Mcpt4), Cathepsin D (Ctsd), and Cathepsin G (Ctsg) are common in mast cell granules (26). No significant changes were observed in the mRNA levels of *Mcpt4* and *Ctsg*, while a 1.6-fold (p=0.031) increase in *Ctsd* in S14-CKO mast cells was observed vs. Samd14-FL/FL, suggesting that mast cell granule content may be changed upon the knockout of Samd14 (Figure 5G).

In summary, Kit loss-of-function and Samd14 loss-of-function mouse models share common phenotypes, including deregulated erythropoiesis and mast cell defects (Figure 5H). The finding in this report and others that Samd14 expression controls RTK signal strength and duration, and opposes apoptotic cell death, may be linked to its role in promoting mast cell differentiation (which requires high Kit signaling) at the expense of other granulocyte lineages. A Samd14 conditional knockout mouse model enables the investigation of Samd14 function and Kit signaling in hematologic diseases. Samd14 knockout may attenuate oncogenic Kit signaling in hematologic diseases including myeloid leukemias, mast cell leukemia, and colorectal / gastric cancers with causative genetic mutations that hyperactivate Kit signaling.

ACKNOWLEDGEMENTS

We would also like to thank the UNMC Flow Cytometry Research Facility, supported by the Nebraska Research Initiative (NRI) and The Fred and Pamela Buffett Cancer Center's National Cancer Institute Cancer Support Grant (P30 CA036727), the UNMC genome engineering core facility (Gurumurthy Channabasavaiah), and the UNMC DNA Sequencing Core, which receives partial support from the National Institute for General Medical Science (NIGMS) INBRE – (P20GM103427–19).

Funding

This study was supported by National Institutes of Health/National Heart, Lung, and Blood Institute [R01 HL155439–01], National Institute of Diabetes and Digestive and Kidney Diseases [K01DK113117–03], funding for K.J.H as a project leader in the Nebraska Center for Molecular Target Discovery and Development [1P20GM121316–01-A1], and a UNMC Graduate Studies Assistantship for M.S.

References

1. Hewitt KJ, Katsumura KR, Matson DR, Devadas P, Tanimura N, Hebert AS, Coon JJ, Kim JS, Dewey CN, Keles S, Paulson RF, and Bresnick EH (2017) GATA Factor-Regulated Samd14 Enhancer Confers Red Blood Cell Regeneration and Survival in Severe Anemia Dev Cell
2. Ray S, Chee L, Zhou Y, Schaefer MA, Naldrett MJ, Alvarez S, Woods NT, and Hewitt KJ (2022) Functional requirements for a Samd14-capping protein complex in stress erythropoiesis. Elife 11
3. Wang X, Zeng W, Kim MS, Allen PB, Greengard P, and Muallem S (2007) Spinophilin/neurabin reciprocally regulate signaling intensity by G protein-coupled receptors. EMBO J 26, 2768–2776 [PubMed: 17464283]
4. Burnett PE, Blackshaw S, Lai MM, Qureshi IA, Burnett AF, Sabatini DM, and Snyder SH (1998) Neurabin is a synaptic protein linking p70 S6 kinase and the neuronal cytoskeleton. Proceedings of the National Academy of Sciences of the United States of America 95, 8351–8356 [PubMed: 9653190]
5. Di Sebastiano AR, Fahim S, Dunn HA, Walther C, Ribeiro FM, Cregan SP, Angers S, Schmid S, and Ferguson SS (2016) Role of Spinophilin in Group I Metabotropic Glutamate Receptor Endocytosis, Signaling, and Synaptic Plasticity. J Biol Chem 291, 17602–17615 [PubMed: 27358397]
6. Ray S, Chee L, Matson DR, Palermo NY, Bresnick EH, and Hewitt KJ (2020) Sterile alpha motif domain requirement for cellular signaling and survival. J Biol Chem
7. Lennartsson J, and Ronnstrand L (2012) Stem cell factor receptor/c-Kit: from basic science to clinical implications. Physiol Rev 92, 1619–1649 [PubMed: 23073628]
8. Garcia-Montero AC, Jara-Acevedo M, Teodosio C, Sanchez ML, Nunez R, Prados A, Aldanondo I, Sanchez L, Dominguez M, Botana LM, Sanchez-Jimenez F, Sotlar K, Almeida J, Escribano L, and Orfao A (2006) KIT mutation in mast cells and other bone marrow hematopoietic cell lineages in systemic mast cell disorders: a prospective study of the Spanish Network on Mastocytosis (REMA) in a series of 113 patients. Blood 108, 2366–2372 [PubMed: 16741248]
9. Ishikawa Y, Kawashima N, Atsuta Y, Sugiura I, Sawa M, Dobashi N, Yokoyama H, Doki N, Tomita A, Kiguchi T, Koh S, Kanamori H, Iriyama N, Kohno A, Moriuchi Y, Asada N, Hirano D, Togitani K, Sakura T, Hagihara M, Tomikawa T, Yokoyama Y, Asou N, Ohtake S, Matsumura I, Miyazaki Y, Naoe T, and Kiyoi H (2020) Prospective evaluation of prognostic impact of KIT mutations on acute myeloid leukemia with RUNX1-RUNX1T1 and CBFB-MYH11. Blood Adv 4, 66–75 [PubMed: 31899799]
10. Beghini A, Peterlongo P, Ripamonti CB, Larizza L, Cairoli R, Morra E, and Mecucci C (2000) C-kit mutations in core binding factor leukemias. Blood 95, 726–727 [PubMed: 10660321]
11. Hirota S, Isozaki K, Moriyama Y, Hashimoto K, Nishida T, Ishiguro S, Kawano K, Hanada M, Kurata A, Takeda M, Muhammad Tunio G, Matsuzawa Y, Kanakura Y, Shinomura Y, and Kitamura Y (1998) Gain-of-function mutations of c-kit in human gastrointestinal stromal tumors. Science 279, 577–580 [PubMed: 9438854]
12. Reith AD, Rottapel R, Giddens E, Brady C, Forrester L, and Bernstein A (1990) W mutant mice with mild or severe developmental defects contain distinct point mutations in the kinase domain of the c-kit receptor. Genes Dev 4, 390–400 [PubMed: 1692559]
13. Ikuta K, and Weissman IL (1992) Evidence that hematopoietic stem cells express mouse c-kit but do not depend on steel factor for their generation. Proceedings of the National Academy of Sciences of the United States of America 89, 1502–1506 [PubMed: 1371359]
14. Broudy VC (1997) Stem cell factor and hematopoiesis. Blood 90, 1345–1364 [PubMed: 9269751]

15. Agosti V, Karur V, Sathyanarayana P, Besmer P, and Wojchowski DM (2009) A KIT juxtamembrane PY567 -directed pathway provides nonredundant signals for erythroid progenitor cell development and stress erythropoiesis. Exp Hematol 37, 159–171 [PubMed: 19100679]

16. Nocka K, Tan JC, Chiu E, Chu TY, Ray P, Traktman P, and Besmer P (1990) Molecular bases of dominant negative and loss of function mutations at the murine c-kit/white spotting locus: W37, Wv, W41 and W. EMBO J 9, 1805–1813 [PubMed: 1693331]

17. Hewitt KJ, Kim DH, Devadas P, Prathibha R, Zuo C, Sanalkumar R, Johnson KD, Kang YA, Kim JS, Dewey CN, Keles S, and Bresnick EH (2015) Hematopoietic Signaling Mechanism Revealed from a Stem/Progenitor Cell Cistrome. Mol Cell

18. Johnson KD, Kong G, Gao X, Hewitt KJ, Sanalkumar R, Prathibha R, Ranheim EA, Dewey CN, Zhang J, Bresnick EH. (2015) Cis-regulatory mechanisms governing stem and progenitor cell transitions. Science Advances 1, e1500503 [PubMed: 26601269]

19. Zhou Y, Dogiparthi VR, Ray S, Schaefer M, Harris HL, Rowley MJ, and Hewitt KJ (2023) Defining A Cohort of Anemia-Activated Cis-Elements Reveals a Mechanism Promoting Erythroid Precursor Function. Blood Adv

20. Quadros RM, Miura H, Harms DW, Akatsuka H, Sato T, Aida T, Redder R, Richardson GP, Inagaki Y, Sakai D, Buckley SM, Seshacharyulu P, Batra SK, Behlke MA, Zeiner SA, Jacobi AM, Izu Y, Thoreson WB, Urness LD, Mansour SL, Ohtsuka M, and Gurumurthy CB (2017) Easi-CRISPR: a robust method for one-step generation of mice carrying conditional and insertion alleles using long ssDNA donors and CRISPR ribonucleoproteins. Genome Biol 18, 92 [PubMed: 28511701]

21. Ohmori S, Moriguchi T, Noguchi Y, Ikeda M, Kobayashi K, Tomaru N, Ishijima Y, Ohneda O, Yamamoto M, and Ohneda K (2015) GATA2 is critical for the maintenance of cellular identity in differentiated mast cells derived from mouse bone marrow. Blood 125, 3306–3315 [PubMed: 25855601]

22. Li Y, Qi X, Liu B, and Huang H (2015) The STAT5-GATA2 pathway is critical in basophil and mast cell differentiation and maintenance. J Immunol 194, 4328–4338 [PubMed: 25801432]

23. Li Y, Gao J, Kamran M, Harmacek L, Danhorn T, Leach SM, O'Connor BP, Hagman JR, and Huang H (2021) GATA2 regulates mast cell identity and responsiveness to antigenic stimulation by promoting chromatin remodeling at super-enhancers. Nat Commun 12, 494 [PubMed: 33479210]

24. Tsai FY, and Orkin SH (1997) Transcription factor GATA-2 is required for proliferation/survival of early hematopoietic cells and mast cell formation, but not for erythroid and myeloid terminal differentiation. Blood 89, 3636–3643 [PubMed: 9160668]

25. Ribatti D, and Crivellato E (2014) Mast cell ontogeny: an historical overview. Immunol Lett 159, 11–14 [PubMed: 24534641]

26. Ohneda K, Moriguchi T, Ohmori S, Ishijima Y, Satoh H, Philipsen S, and Yamamoto M (2014) Transcription factor GATA1 is dispensable for mast cell differentiation in adult mice. Mol Cell Biol 34, 1812–1826 [PubMed: 24615013]

27. Valent P, Spanblochl E, Sperr WR, Sillaber C, Zsebo KM, Agis H, Strobl H, Geissler K, Bettelheim P, and Lechner K (1992) Induction of differentiation of human mast cells from bone marrow and peripheral blood mononuclear cells by recombinant human stem cell factor/kit-ligand in long-term culture. Blood 80, 2237–2245 [PubMed: 1384799]

28. Dahlin JS, Hamey FK, Pijuan-Sala B, Shepherd M, Lau WWY, Nestorowa S, Weinreb C, Wolock S, Hannah R, Diamanti E, Kent DG, Gottgens B, and Wilson NK (2018) A single-cell hematopoietic landscape resolves 8 lineage trajectories and defects in Kit mutant mice. Blood 131, e1–e11 [PubMed: 29588278]

29. Lantz CS, Boesiger J, Song CH, Mach N, Kobayashi T, Mulligan RC, Nawa Y, Dranoff G, and Galli SJ (1998) Role for interleukin-3 in mast-cell and basophil development and in immunity to parasites. Nature 392, 90–93 [PubMed: 9510253]

30. Durand B, Migliaccio G, Yee NS, Eddleman K, Huima-Byron T, Migliaccio AR, and Adamson JW (1994) Long-term generation of human mast cells in serum-free cultures of CD34+ cord blood cells stimulated with stem cell factor and interleukin-3. Blood 84, 3667–3674 [PubMed: 7524746]

31. Teng LKH, Pereira BA, Keerthikumar S, Huang C, Niranjan B, Lee SN, Richards M, Schittenhelm RB, Furic L, Goode DL, Lawrence MG, Taylor RA, Ellem SJ, Risbridger GP, and Lister NL (2021) Mast Cell-Derived SAMD14 Is a Novel Regulator of the Human Prostate Tumor Microenvironment. Cancers (Basel) 13

32. Costa JJ, Demetri GD, Harrist TJ, Dvorak AM, Hayes DF, Merica EA, Menchaca DM, Gringeri AJ, Schwartz LB, and Galli SJ (1996) Recombinant human stem cell factor (kit ligand) promotes human mast cell and melanocyte hyperplasia and functional activation in vivo. J Exp Med 183, 2681–2686 [PubMed: 8676090]

33. Ho CCM, Chhabra A, Starkl P, Schnorr PJ, Wilmes S, Moraga I, Kwon HS, Gaudenzio N, Sibilano R, Wehrman TS, Gakovic M, Sockolosky JT, Tiffany MR, Ring AM, Piehler J, Weissman IL, Galli SJ, Shizuru JA, and Garcia KC (2017) Decoupling the Functional Pleiotropy of Stem Cell Factor by Tuning c-Kit Signaling. Cell 168, 1041–1052 e1018 [PubMed: 28283060]

34. da Silva EZ, Jamur MC, and Oliver C (2014) Mast cell function: a new vision of an old cell. J Histochem Cytochem 62, 698–738 [PubMed: 25062998]

Highlights

- Samd14 deletion caused more severe anemia after 5-fluorouracil-induced stress
- Mast cell differentiation was attenuated in Samd14-CKO cells.
- Samd14-CKO mast cells were functionally impaired and less reactive to SCF and IL-3
- Samd14-CKO mice were similar to other Kit loss-of-function mouse models

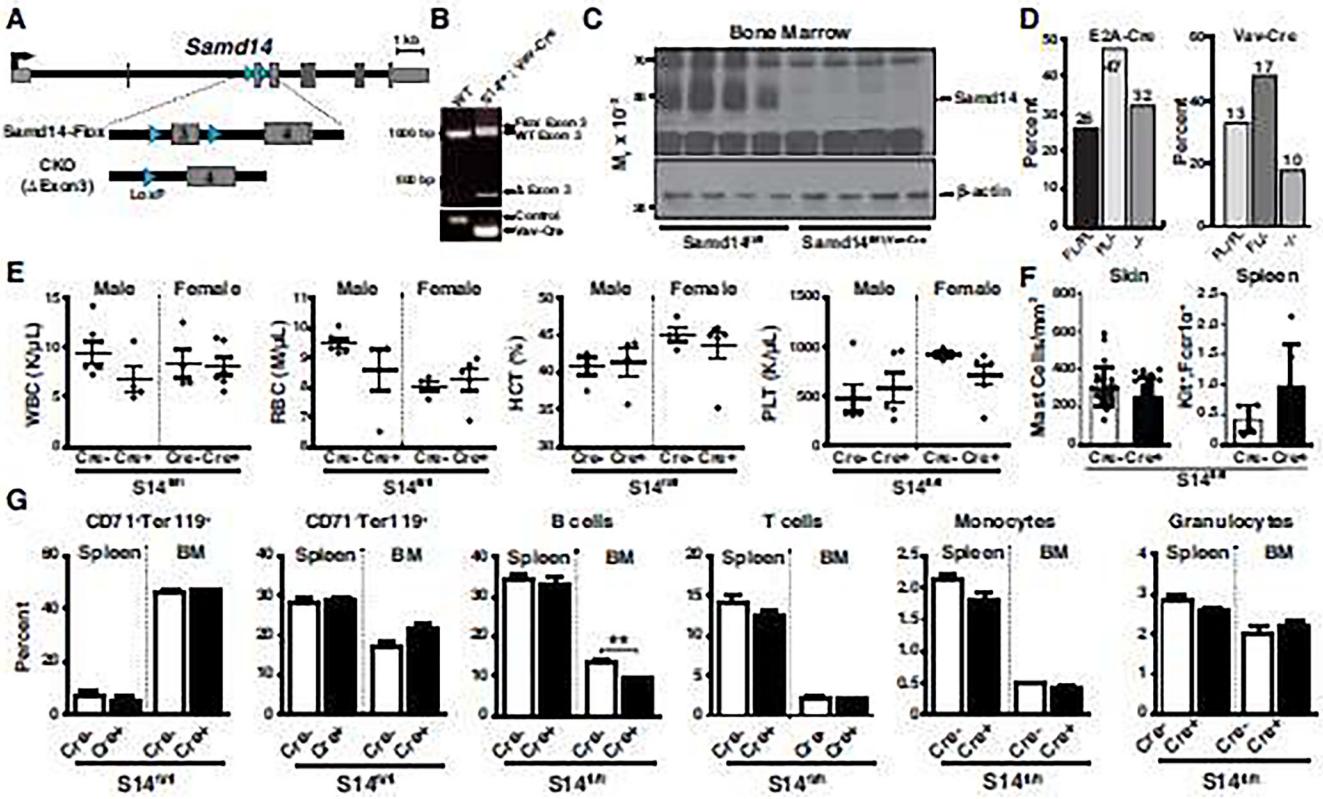

Figure 1: Conditional knockout of Samd14 does not alter steady-state hematopoiesis.

A) Floxed intron 3 at the Samd14 locus. B) Agarose gel electrophoresis of PCR-amplified regions flanking Samd14 exon 3 and the Vav-Cre gene in WT and Samd14$^{Fl/+}$; Vav-Cre mice. C) Western blotting analysis of Samd14 protein in total bone marrow cells isolated from Samd14$^{fl/fl}$ (WT) or Samd14$^{fl/fl;Vav\text{-}Cre}$ (Mut) mice (N=4). D) Percentages of offspring genotyped (total numbers above each bar) at 3 weeks old in germline-deleted Samd14 and conditionally deleted (Vav-Cre) knockout. E) Complete blood count analysis of hematologic parameters in 8-week-old mice WBC=white blood cells, RBC=Red blood cells, HCT=Hematocrit, PLT=Platelet. WT (n=9) and Mut (n=4–6). F) Quantitation of mast cells/mm^2 in ear skin (counted using toluidine blue stain) and percentage of Kit$^+$Fcer1a$^+$ cells in spleen (counted by flow cytometry). G) Quantitation of erythroid (CD71$^+$Ter119$^+$ and CD71$^-$Ter119$^+$), B cell (CD19$^+$), T cell (thy1$^+$), Monocyte (Mac1$^+$) and granulocyte (Gr1$^+$) cells in total bone marrow.

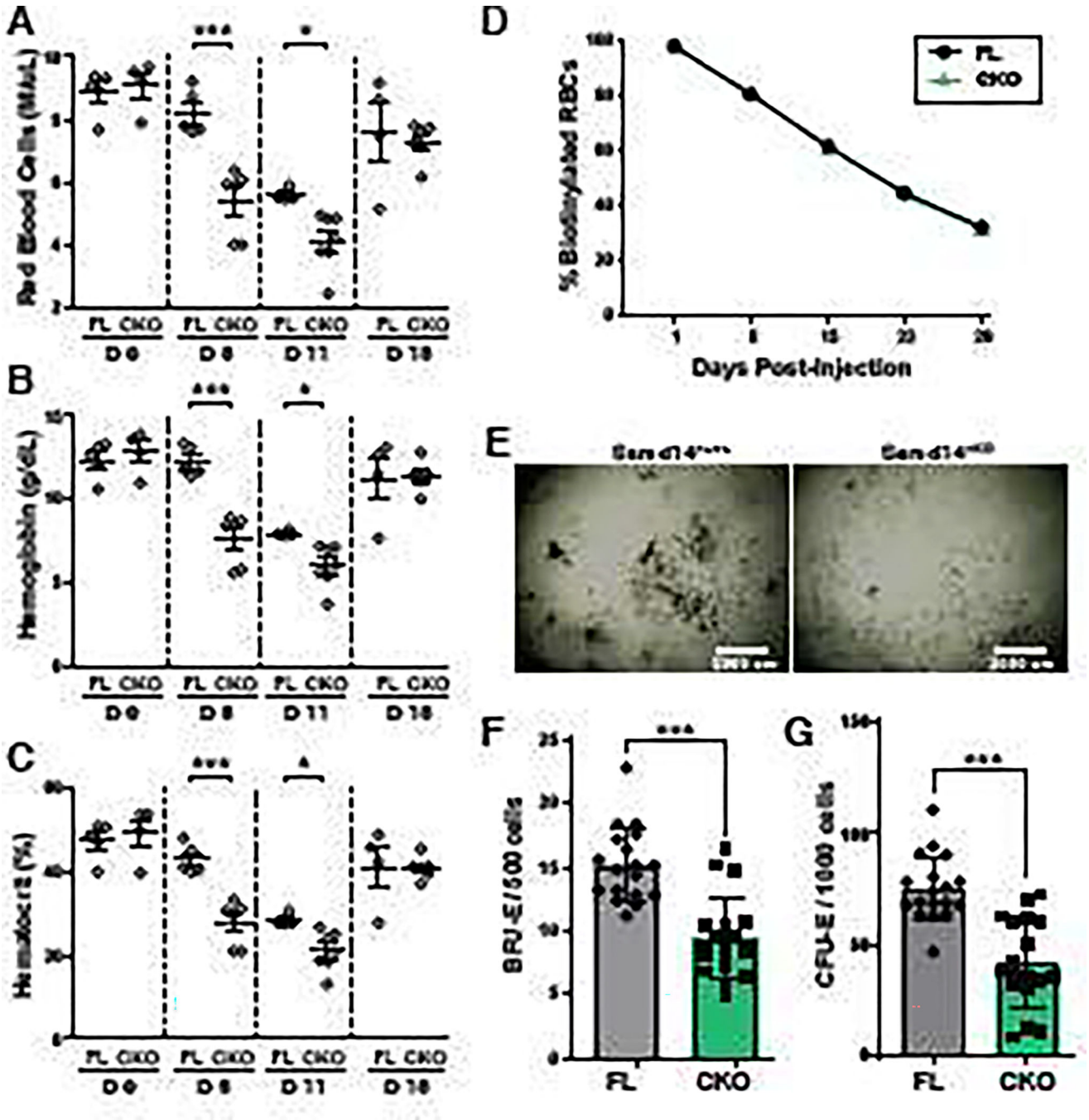

Figure 2: Erythropoietic regeneration is impaired in Samd14 CKO mice following hematopoietic stress in

A) Red blood cells (M/uL) in peripheral blood at indicated time points following 250 mg/kg 5-FU in Samd14-FL/FL and Samd14-CKO mice. B) Hemoglobin (g/dL) in peripheral blood at indicated time points following 250 mg/kg 5-FU treatment of Samd14-FL/FL and Samd14-CKO mice. C) Hematocrit (%) in peripheral blood at indicated time points following 250 mg/kg 5-FU treatment of Samd14-FL/FL and Samd14-CKO mice. D) Biotinylation of red blood cells via retro-orbital injection was monitored by flow cytometry and represented as a percentage of total $Ter119^{+}$ cells in peripheral blood. E) Representative

images of colonies formed from total bone marrow isolated 10 days after 5-FU injection. F) Quantitation of burst forming unit-erythroid (BFU-E) from Samd14-FL/FL and Samd14-CKO cells isolated from total bone marrow 10 days after 5-FU injection. G) Quantitation of colony forming unit-erythroid (CFU-E) from Samd14-FL/FL and Samd14-CKO cells isolated from total bone marrow 10 days after 5-FU injection.

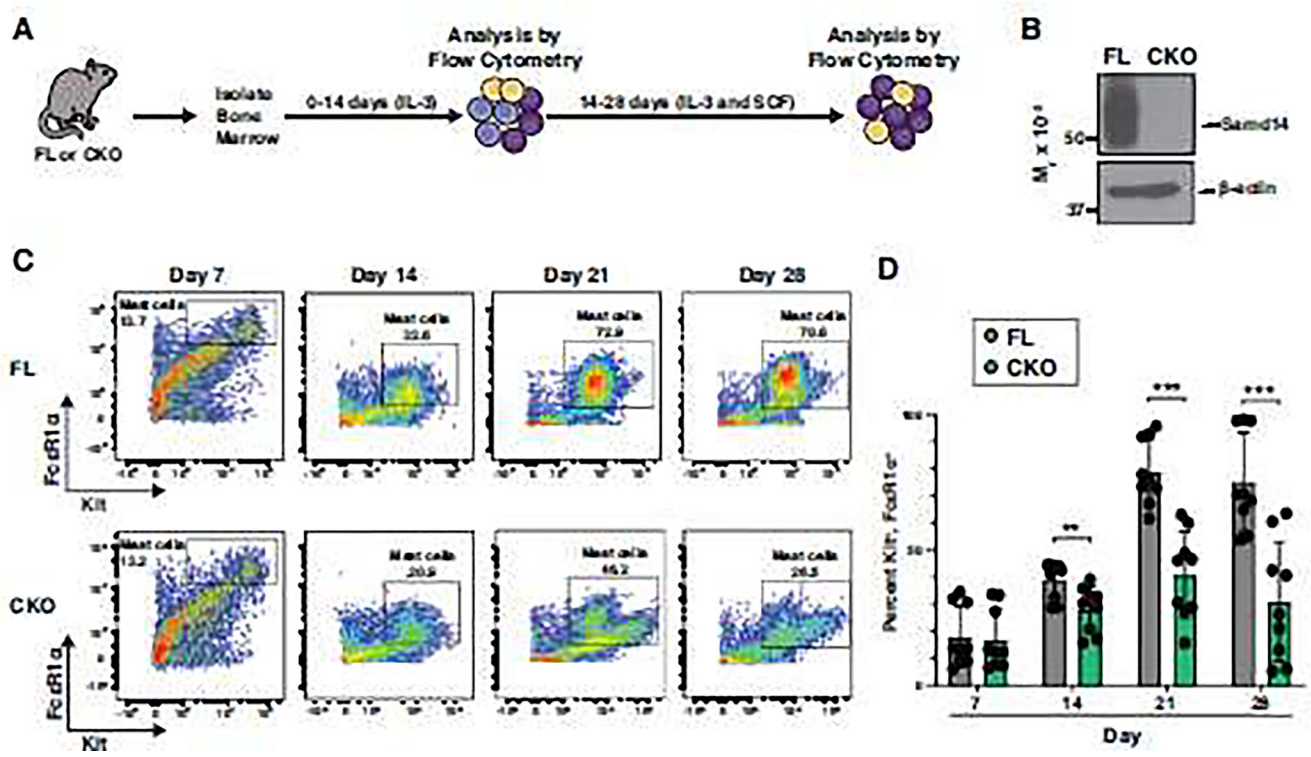

Figure 3: Samd14 knockout impairs ex vivo mast cell differentiation.

A) Schematic outlining 28-day mast cell differentiation (light purple cells=HSPCs) (yellow cells=monocytes/granulocytes) (dark purple cells=mast cells). B) Western blot of Samd14 and β-actin in sorted mast cells (n=3). C) Representative flow cytometry plot of anti-FcƐr1α APC and anti-Kit Pe-Cy7 at day 7, 14, 21, and 28 of mast cell differentiation. Cells were first gated for live cells (DAPI−). D) Quantitation of mast cell (Kit+ FcƐr1α+) numbers at day 7, 14, 21, and 28 of total bone marrow culture as determined by flow cytometry (n=9). Error bars represent SD. **p<.01, ***p<.001, (two-tailed unpaired Student's t test).

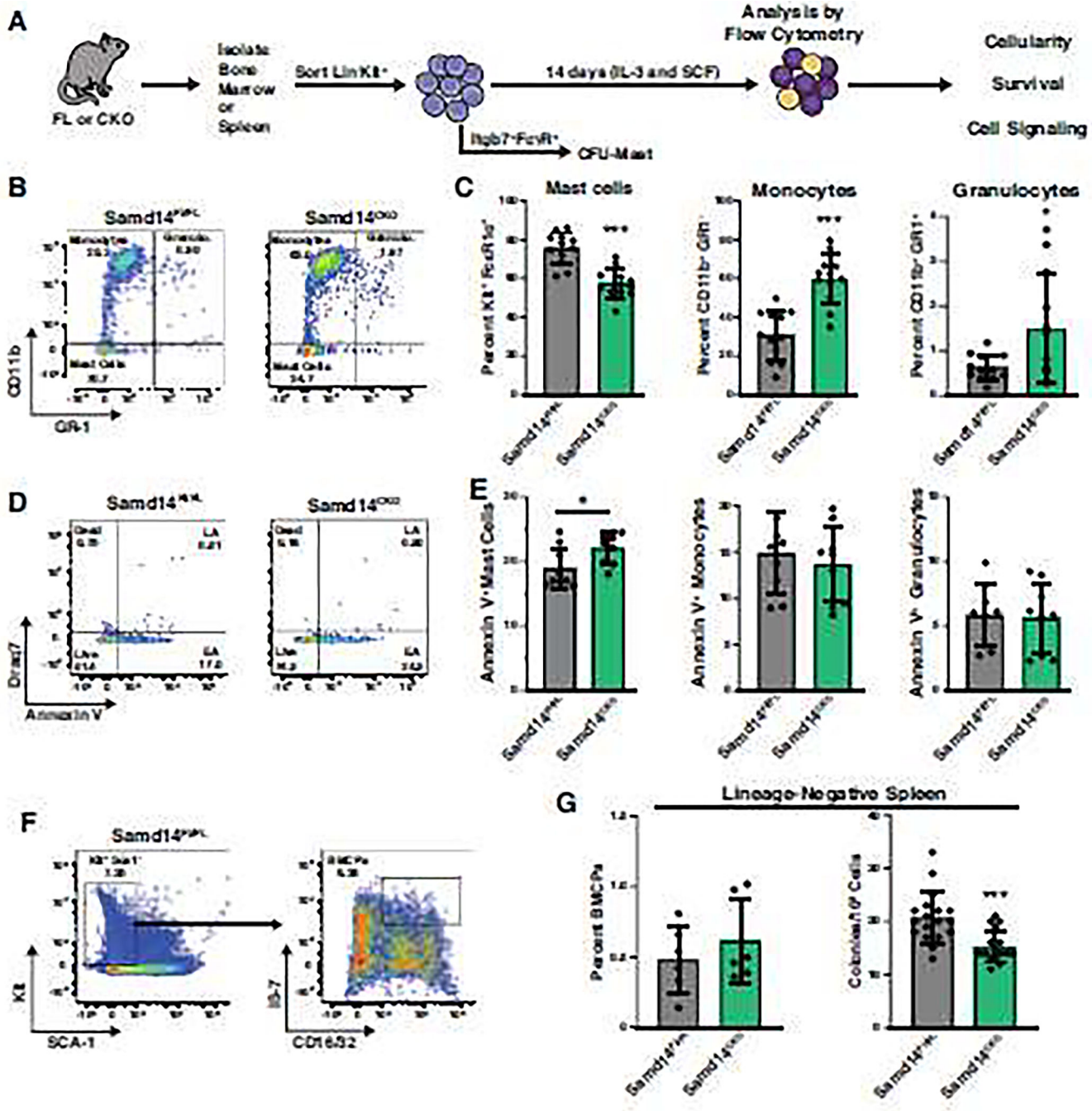

Figure 4: Absence of Samd14 results in mast cell defects.

A) Schematic outlining 14-day mast cell differentiation and BMCP isolation. B) Representative flow cytometry scatter plot of anti-CD11b PE and anti-GR-1 brilliant violet 711 at day 14 of mast cell differentiation (Granulo.=granulocytes). Cells were first gated for live cells (DAPI−). C) Quantitation of mast cell (Kit^+ $Fc\varepsilon r1\alpha^+$), monocyte ($CD11b^+$ $Gr1^-$), and granulocyte (CD11b+, GR-1+) percentages at day 14 of Kit+ bone marrow culture as determined by flow cytometry (n=12). D) Representative flow cytometry scatter plot of membrane-impermeable Draq7 and anti-Annexin V (AnnV) Pacific Blue. Cells were

first gated for mast cells (Kit+ FcƐr1α+), monocytes (CD11b+ GR-1−), or granulocytes (CD11b+, GR-1+). Live=AnnV− Draq7−; Early apoptotic (EA)=AnnV+ Draq7−; Late apoptotic (LA)=AnnV+ Draq7+; Dead=AnnV− Draq7+. E) Quantitation of percent early apoptotic mast cells, monocytes, and granulocytes at day 7 of Kit+ bone marrow culture. F) Representative flow cytometry scatter plots of BMCP isolation gating strategy anti-Kit Pe-Cy7, anti-SCA-1 PerCp-Cy5.5 and anti-CD16/32 PE, anti-Integrin-β7 FITC.G) Quantitation of percent BMCPs in Lin- spleens (left) (n=6)and BMCPs grown for 7 days and quantitated (right) (n=18). Error bars represent SD. *p<.05, ***p<.001 (two-tailed unpaired Student's t test).

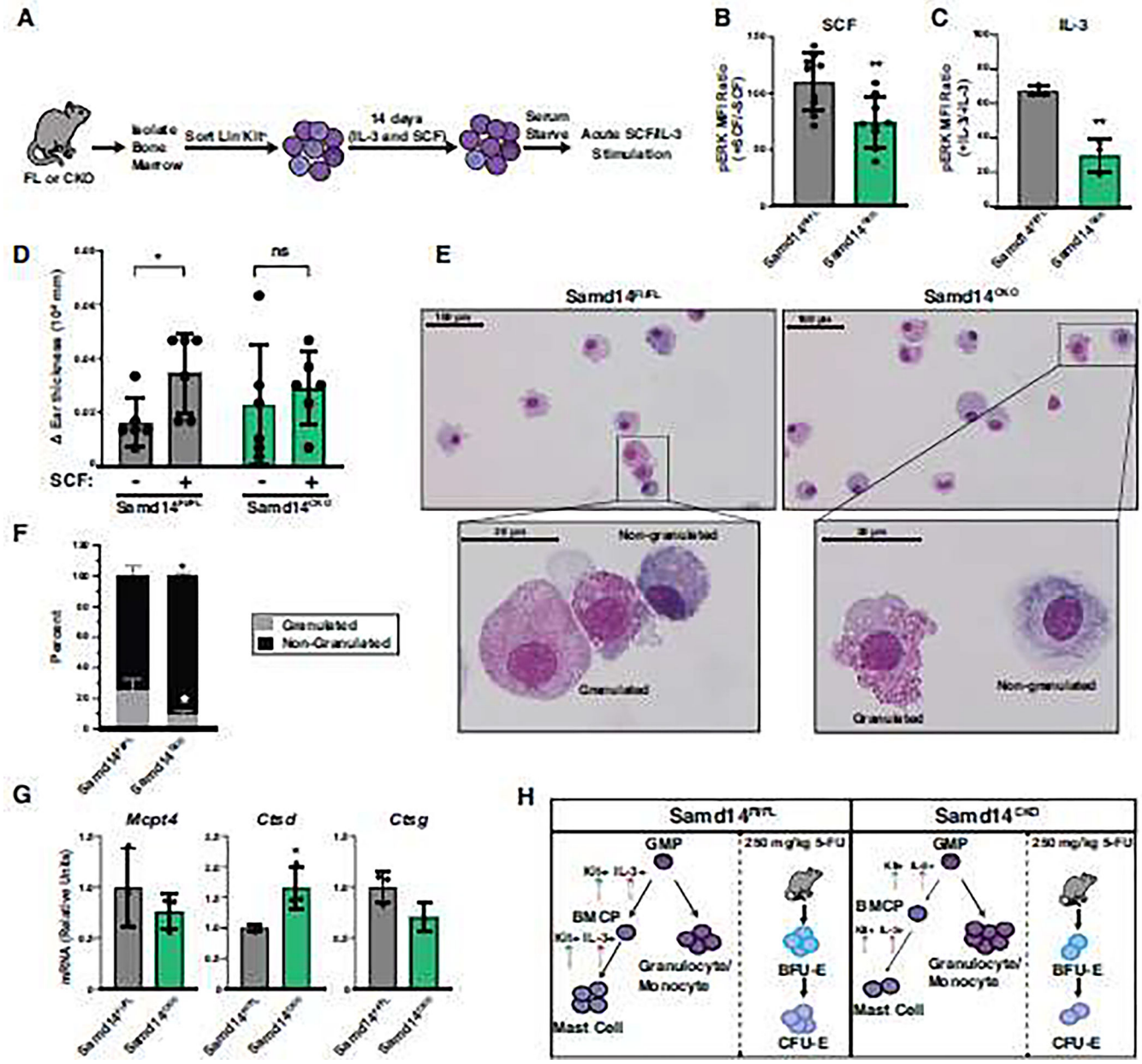

Figure 5: Samd14 knockout causes defects in mast cell function.

A) Schematic outlining the mast cell acute stimulation strategy. B) Quantitation of the fold-change of pERK median fluorescent intensity in SCF-treated samples over vehicle-treated controls at 5 min post-SCF stimulation. C) Quantitation of the fold-change of pERK median fluorescent intensity in IL-3-treated samples over vehicle-treated controls at 5 min post-IL-3 stimulation. D) Change in ear thickness of mice injected with PBS alone (left ear pinnae) or PBS containing 50 μg/mL SCF (right ear pinnae). Ear thickness was measured before injection and then 2 hours post-injection. The change in ear thickness was determined from the post-injection ear measurement minus the initial ear thickness measured for each ear (n=6). E) Representative images of Wright-Giemsa stained mast cells at 14 days of Kit+ bone marrow culture (40x-magnification).F) Quantitation of granulated and non-granulated

mast cell percents as determined from Wright-Giemsa stained mast cells (n=3). G) mRNA levels of mast cell protease 4 (Mcpt4) Cathepsin D (Ctsd), and Cathepsin G (Ctsg) in mast cells. Normalized to 18S rRNA (n=3). H) Model of Samd14-CKO phenotype. Error bars represent SD. *p<.05, **p<.01 (two-tailed unpaired Student's t test).